Proceedings of the 16th International Conference on Soil Mechanics and Geotechnical Engineering

doi:10.3233/978-1-61499-656-9-659

SPT sampler static penetration resistance in the case of a sandy soil

Résistance statique du système sol et tube carottier SPT dans un sol sableux

N. Aoki, E.R. Esquivel, L.F.S. Neves & J.C.A. Cintra
Department of Geotechnical Engineering, University of Sao Paulo, Sao Carlos, Brazil

ABSTRACT

This paper describes the performance of static load tests on the SPT sampler in sandy soils. The tests were performed soon after the measurements of the N_{SPT} index and the energy applied. It has been verified that the deformation potential energy assessed by the static test load-settlement curve is nearly equal to the work done by the system. Under these conditions, the efficiency based on the work done by the system non-conservative forces could be directly evaluated from the results of static load tests performed on the sampler.

RÉSUMÉ

Cet article présente des essais de chargement statique sur le tube carottier du SPT dans des sols sableux. Les chargements ont été réalisés tout de suite après les mesures du nombre de coups N_{SPT} et de l'énergie transmise. Il a été de plus vérifié que la valeur de l'énergie de déformation potentielle représentée par la courbe charge x tassement de l'essai statique est presque égale à la valeur du travail dissipé par le systéme. Dans ces conditions, l'efficacité obtenue d'après le travail dissipé par les forces non-conservatives du système peut aussi être évaluée directement à partir des résultats d'essais de chargement statique réalisés sur le tube carottier du SPT.

1 INTRODUCTION

The Standard Penetration Test (SPT) is an in-situ test widely used in Brazil and in many countries in the world.

The evaluation of the energy arriving to the SPT sampler is traditionally done by means of sensors installed in the upper part of the SPT apparatus rod. The first compression wave is integrated over the time required for the wave to reach the sampler top. In this approach, the efficiency increases with the increase of the rod length, as demonstrated by Schmertmann e Palacios (1979). However, this seems to be in opposition to the common sense.

Because of that, Aoki and Cintra (2000) have redefined the SPT efficiency based on the deformation potential energy curve corresponding to the sampler top. This energy is numerically equal to the kinetic energy in this section. According to Hamilton's Principle (Aoki, 1997), at the end of the hammer impact (after the system has been discharged), the deformation potential energy is transformed into elastic deformation potential energy and work done by the non conservative resisting forces. The work is numerically equal to the area enclosed by the loading and unloading branches of the resistance-displacement curve at the sampler top. In addition, the SPT efficiency is represented by the work done during the sampler penetration, soon after the impact, divided by the available potential energy before the impact. On the other hand, the work is equal to the product of the resisting force by the permanent displacement. As a consequence, since the work and the displacement are known, the resisting force developed during the sampler penetration can be computed.

According to Abou-Matar et al. (1996), at every impact instant, the resisting force depends on the displacement (static resisting force), the velocity (damping force) and the acceleration (inertial force) developed during the impact elapsed time. In this model, for sandy soils, the inertial and damping components are negligible, resulting that the resisting force magnitude will be nearly the same as the static component magnitude.

To verify these propositions, Neves (2004) performed a series of Standard Penetration Tests in a non-saturated sandy soil field, in Araras, Brazil. The readings of the traditional N-value or N_{SPT} index were complemented with readings of the kinetic energy. The measurement of the kinetic energy was performed with the SPT Analyzer®, through sensors installed at the sampler top. Immediately after the determination of the N_{SPT} index, a static load test was performed by applying an increasing static load on the rods-SPT sampler set. The SPT truck was used as the reaction frame.

The dynamic and static load test analyses have shown that: a) in both cases, nearly all the system deformation energy was transformed into non-conservative resisting forces work; b) the measured kinetic energy in the dynamic test is numerically the same as the deformation energy computed as the area under the static test load-displacement curve; c) the magnitude of the sampler penetration resisting force, evaluated from the measured work in the dynamic test, is equal to the magnitude of the applied load in the static test, corresponding to the maximum displacement in the dynamic test.

From the above results, it has been concluded that: a) the work done by the system, assessed from the static load test on the sampler, allows the evaluation of the impact efficiency; b) it is possible to convert the N_{SPT} resistance index into a sampler penetration resisting force at the test depth.

2 RESISTING FORCE DEVELOPED DURING THE SAMPLER PENETRATION

The resisting force (R_s) developed during the sampler penetration, corresponding to the N_{SPT} index is given by:

$$R_s = \frac{T_A \times N_{SPT}}{0.3} \quad \text{(kN)} \tag{1}$$

or

$$R_s = \frac{\eta^* \times 0.478 \times N_{SPT}}{0.30} \text{ (kN)} \quad (2)$$

where T_A = maximum transferred energy to the top of the set sampler-soil; 0.478 kJ = nominal SPT energy; η* = efficiency, measured at the top section, according to the definition suggested by Aoki and Cintra (2000).

$$\eta^* = \frac{T_A}{478\,J} \times 100 \ (\%) \quad (3)$$

The N_{SPT} resistance index can be transformed into an equivalent static resisting force through Equation 2, if the average efficiency expressed by Equation 3 is known. Therefore, the N_{SPT} resistance index can be considered as a parameter with determined physical meaning. Finally, for resilient soils, Equation 3 can be re-written:

$$\eta^* = \frac{W_A}{478\,J} \times 100 \ (\%) \quad (4)$$

where W_A = work done by the non-conservative resisting forces.

3 STATIC LOAD TEST

The testing equipment, used to perform the static tests with maintained load, consists of a load cell, a hydraulic jack, a ball joint and a pair of dial indicators and acrylic plates. The load cell has a reading accuracy of 0.1 kN.

Figure 1 shows the equipment assemblage schematics for SPT energy measurement and for static load test, performed after the last sampler dynamic penetration.

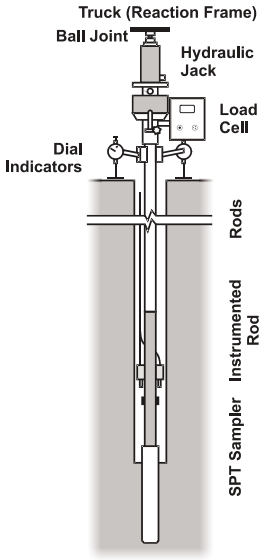

Figure 1. Schematics for SPT energy measurement and for static load test

Before starting the static load test, the static resistance R_s was assessed by means of Equation (1). The apparatus was assembled and an initial load was applied to the system. After that, it was assumed that the displacement was zero. Then, the load was increased in variable increments until its magnitude reached 2/3 of R_s. After that, all load increments were constant and equal to 0.1 kN. For each load step, displacement readings were performed every minute, until the difference between two consecutive readings was less than 0.5 mm. Then, the next load step was applied.

The deformation energy magnitude was estimated from the load-settlement curve obtained from the static load tests. This was accomplished by performing the static load tests so that at least one sampler settlement was equal to the dynamic penetration magnitude corresponding to the last hammer impact, when obtaining the N_{SPT} index. After the specified minimum displacement was reached, the system was unloaded in variable steps. Since the instrumented rod is not waterproof, all tests were performed above water level, in order to prevent electronics malfunctioning.

Figure 1 shows that the instrumented rod is located just above the SPT sampler. In such way, it is possible to measure the kinetic energy T_A reaching the sampler, which is transformed into deformation energy during the sampler penetration into the soil. The use of the truck as a reaction frame is an economical way to perform the tests. However, any reaction system can be used, since it is consistent with the anticipated R_s magnitude.

4 TEST RESULTS: DATA ANALYSIS AND DISCUSSION

4.1 *Standard Penetration Test results*

The N_{SPT} indexes have been evaluated at every depth meter at the test sites.

Table 1 shows the N_{SPT} index and the average penetration for one impact. It should be noticed that in practice it is usual to round the penetrations to 30 cm.

Table 1. SPT results

Case	Site	Depth (m)	SPT ID	N_{SPT} Measured	Average Penetration (mm)
1	Araras 1	6.0	SP 05	7/27	39
2	Araras 3	4.0	SP 02	4/28	70
3	Araras 4	6.0	SP 01	6/32	53
4	Araras 4	7.0	SP 01	6/28	47
5	Araras 4	8.0	SP 01	7/29	41

4.2 *Dynamic test results*

Table 10 shows the magnitudes of the kinetic energy T_A, corresponding to the last impact in each SPT measurement, the measured maximum axial force in the instrumented rod (F_{max}) and the magnitude of the sampler permanent penetration into the soil (S).

Table 2. Dynamic test results.

Case	T_A (J)	F_{max} (kN)	S (mm)
1	263	119	35
2	214	107	60
3	180	98	55
4	146	98	46
5	166	90	33

4.3 *Static load test results*

Figure 2 shows the load-settlement curves corresponding to static load tests. This graphs show that the unloading curve, starting from the maximum applied load, is nearly horizontal. This means that all deformation energy stored by the system up

to this load level is transformed into work done by non-conservative resisting forces during the unloading phase.

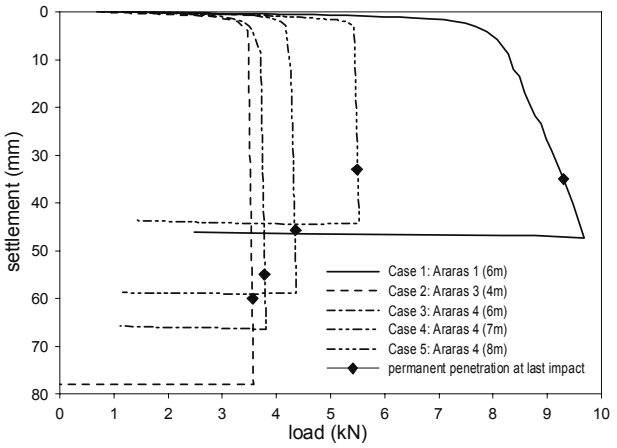

Figure 2. Static load test results.

The diamond symbol on the static load test curve is defined by a settlement (ρ) equal to the permanent penetration corresponding to the last impact (values shown in Table 2), and by the corresponding load on the static test curve.

Table 3 shows the maximum load (P_{max}) and the corresponding settlement (ρ_{max}), the settlement equal to the permanent penetration corresponding to the last impact, and the deformation energy V_A, which is numerically equal to the area under the loading curve up to settlement qual to ρ.

Table 3. Static load test results

Case	P_{max} (kN)	ρ_{max} (mm)	ρ (mm)	V_A (J)
1	9.7	47.3	35	295
2	3.6	78.0	60	209
3	3.8	66.5	55	202
4	4.4	59.0	46	193
5	5.5	44.2	33	177

4.4 *Test data analysis*

Figure 3 shows a comparison between the kinetic energy T_A, measured during the dynamic test and the deformation energy V_A, obtained from the static load test.

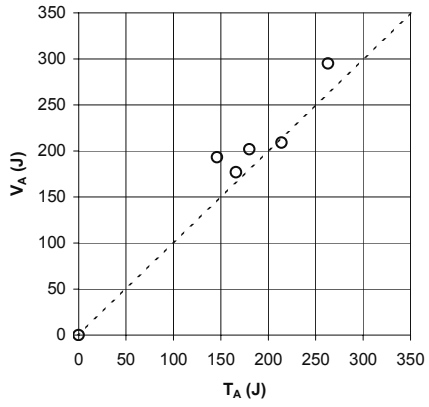

Figure 3. Comparison between the kinetic energy T_A and the deformation energy V_A

The graph shows that the deformation energy V_A is greater than the kinetic energy T_A. One possible reason is that the static load test was preceded by a dynamic load test, which caused a significant additional sampler penetration into the soil, changing the static test initial conditions. Table 4 shows the efficiency values evaluated from the work done by the non-conservative forces, according to Equation 3.

It can be observed that: a) the static efficiency is slightly higher than the dynamic one, similarly to what happened with the energy values (see Figure 3), for the same reason; b) these efficiency values are low when compared to the values usually obtained in the Brazilian practice.

Table 4. Estimated efficiencies in terms of work done in the dynamic test and in the static test.

Case	W_A (dynamic) (J)	W_A (static) (J)	η^* (dynamic) (%)	η^* (static) (%)
1	263	295	55	62
2	214	209	45	44
3	180	202	38	42
4	146	193	31	40
5	166	177	35	37

Belincanta (1998) has found that for a 14 m long rod, the average efficiency is 73%, and that extrapolating the values for a longer rods, the average efficiency will be 81.9%, very close to that one obtained by Cavalcante (2002). The average efficiency value obtained by Cavalcante (2002), for rods whose length vary from 2 to 14 m and N_{SPT} ranging from 2 to 64, was 82.3%.

Table 4 confirms that it is also possible to evaluate the impact efficiency from the work done during the static load test on the SPT sampler. Table 5 shows the static resistance values assessed through Equations 1 and 2, using the efficiency values shown in Table 4 and the measured values in the static load tests, for static displacements equal to displacements measured in the dynamic test.

Table 5. Static resistance values: estimated and measured in the static load test.

Theoretical N_{SPT}	Displ. (mm)	R_s (eq. 2) (kN)	R_s (eq. 1) (kN)	R_s (measured) (kN)
7.78	35	6.82	7.51	9.30
4.29	60	3.06	3.57	3.56
5.63	55	3.38	3.27	3.78
6.43	46	3.13	3.17	4.35
7.24	33	4.01	5.03	5.49

The value of the measured N_{SPT} index can be found in the fifth column of Table 1. The first column of Table 5 shows the same value in the format of a theoretical N_{SPT} index equivalent to a penetration of 30 cm.

Table 5 corroborates that it is possible to convert the N_{SPT} index into a sampler penetration resistance at test depth.

Figure 4 shows a comparison between the static resistance values, assessed with Equations 1 and 2, and the measured values in the static load tests. This figure also shows the static resistance values evaluated with the DINEXP-1D software, as presented by Cavalcante (2002), assuming an efficiency η^* equal to 70%.

There is a lack of data corresponding to the resistance range from 20 to 80 kN, as a consequence of the particular conditions of the sites where the tests were performed. Figure 5 shows a magnified version of Figure 4.

It can be observed that the measured resistance in the static load test is slightly higher than those assessed through Equations 1 and 2.

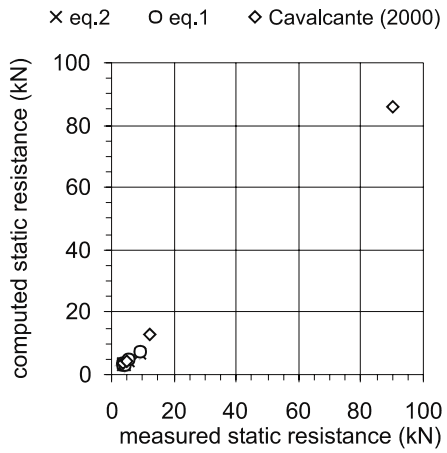

Figure 4. Comparison between the estimated resistance and the measured resistance in the static load test.

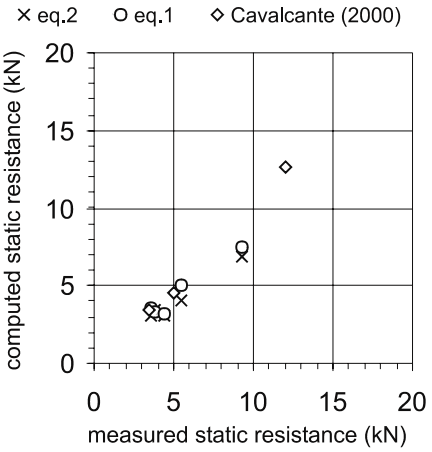

Figure 5. Comparison between the estimated resistance and the measured resistance in the static load test (closer view).

5 CONCLUSIONS

The previously described static load test with the SPT rod-sampler setup was performed for the first time in the world by Neves (2004). From the data analysis and comparison with the data obtained using the SPT Analyzer, regarding unsaturated sandy soils, the following conclusions can be inferred:

- The application of the Hamilton's Principle to energy transformations occurred during the hammer impact Standard Penetration Tests could be verified.
- The deformation energy and the efficiency obtained in static load tests are greater than the kinetic energy and the efficiency determined in the dynamic test. The reason for this is that the static load test was preceded by the dynamic test.
- It is possible to transform the NSPT index into static resistance, using Equations 1 and 2.
- The static resistance evaluated through the suggested expressions is slightly lesser than that one assessed in the static load test.
- The static load tests show that the deformation energy stored in the system has been transformed into work done by non-conservative resisting forces.
- The efficiency values measured with the automatic equipment correspond to 80% of those found in the Brazilian practice.
- It is possible to evaluate the impact efficiency from the work done during the static load test on the SPT sampler.

Finally, the necessity of additional researches should be emphasized to confirm the applicability of the previously described procedures in this paper, for different kinds of soils. In addition, tests performed below the water level should be considered.

ACKNOWLEDGMENTS

The authors are very thankful to Fundacao Jose Bonifacio (FUJB) and to COPPE/UFRJ for the loan of the SPT Analyzer. Moreover, they would like to express their recognition to the companies EG Barreto and Solum for the loan of the sounding equipment and support during the performance of the static load tests.

REFERENCES

Abou-Matar, H.; Rausche, F.; Thendean, G.; Likins, G.; Goble, G. 1996. Wave equation soil constants from dynamic measurements on SPT, *Fifth International Conference on the Application of Stress-Wave Theory to Piles*, Orlando, p. 163-175.

Aoki, N, (1997). Assessment of the ultimate load capacity for driven piles in dynamic load test with increasing energy (in Portuguese), *Ph.D. Dissertation*, University of Sao Paulo, Sao Carlos, 111 p.

Aoki, N; Cintra, J.C.A. (2000). The application of energy conservation Hamilton's Principle to the determination of energy efficiency in SPT tests, *VI International Conference on the Application of the Stress-Wave Theory to Piles*, Sao Paulo, p. 457-460.

Belincanta, A. (1998). Evaluation of intervenient factors on the SPT penetration resistance index (in Portuguese), *Ph.D. Dissertation*, University of Sao Paulo, Sao Paulo, 141 p.

Cavalcante, E.H. (2002). Theoretical-experimental investigation on SPT (in Portuguese), *Ph.D. Dissertation*, COPPE / Federal University of Rio de Janeiro, Rio de Janeiro, 441 p.

Costa, A.M. (1978). DINEXP-1D (in Portuguese). Software developed at CENPES/Petrobras, *Petrobras*, Rio de Janeiro.

Neves, L.F.S. (2004). A methodology for the determination of the Standard Penetration Test efficiency through the static load test on SPT sampler (in Portuguese). *M.Sc. Thesis*, University of Sao Paulo, Sao Carlos.

Schmertmann, J.H.; Palacios, A. (1979). Energy Dynamics of SPT, *Journal of Soil Mechanics and Foundation Division, ASCE, v. 105, n° GT8, p. 909-926.*